

Influence of material processing on crystallographic and electrochemical properties of cobalt-free $\text{LaNi}_{4.95}\text{Sn}_{0.3}$ hydrogen storage alloy

WEI Fan-song(魏范松)¹, LEI Yong-quan(雷永泉)¹, CHEN Li-xin(陈立新)¹,
YING Tiao(应 窈)¹, GE Hong-wei(葛红卫)¹, LÜ Guang-lie(吕光烈)²

1. Department of Materials Science and Engineering, Zhejiang University, Hangzhou 310027, China;

2. Central Laboratory, Zhejiang University, Hangzhou 310028, China

Received 22 August 2005; accepted 15 November 2005

Abstract: The effects of the alloy preparation methods, including the conventional casting, annealing and melt-spinning, on the crystallographic and electrochemical properties of the Co-free $\text{LaNi}_{4.95}\text{Sn}_{0.3}$ alloy samples were investigated. The results reveal that the as-cast alloy consists of a main phase of CaCu_5 -type structure and a little second phase (Sn) with noticeable composition segregation and rather poor cycling stability ($S_{200}=40.1\%$). While the annealed and melt-spun alloys are of single CaCu_5 -type structure phase with a more homogeneous composition and lower cell volume expansion rate ($\Delta V/V$) on hydriding, and a dramatically improved cyclic stability ($S_{200}=73.6\%–76.2\%$), although their activation rate, initial capacity and high-rate dischargeability are lowered somewhat. It is found that the decrease in both the electrocatalytic activity and the hydrogen diffusion rate of the annealed and melt-spun alloys is the main cause for their relatively lower high-rate dischargeability, and the improved cycling stability is due to their lower volume expansion on hydriding and more uniform composition.

Key words: hydrogen storage alloy; Co-free alloy; material processing; crystal structure; electrochemical property

1 Introduction

Mischmetal-based AB_5 -type alloys containing about 10% Co (mass fraction) are now widely used as the negative electrode materials of Ni/MH batteries because of their long cycle life and good overall properties. It is known that Co is an essential element for suppressing the pulverization and corrosion of the alloys during charge/discharge cycling, which enhances the cycle life[1,2]. However, Co is expensive and drastically increases the alloy cost. Therefore, in order to reduce the alloy cost, much work on the substitution of Co with other low-cost elements (Cu, Fe, Si, Sn, etc) has been carried out, and several low-Co or Co-free alloys were developed[3–5]. However, for commercial applications the cycling stability and overall electrode properties of these alloys have to be improved further. It has been found that the use of overstoichiometric alloys (AB_{5+x}) is a promising way to reduce the alloy pulverization[6–8], and the cycling stability of the AB_5 alloys with different Co contents can also be improved by different material

processing methods such as heat treatment[9,10] and rapid solidification process[11–13]. However, it appears that the influence of alloy composition and preparation methods on the cycling performance is quite complex and not very clear yet. In addition, for the recently reported Co-free $\text{La}(\text{Ni}, \text{Sn})_{5+x}$ alloys[2,14], which has been considered a new class of Co-free alloys due to their simple composition and good storage capacity, no farther information on the effects of the material processing methods on the electrochemical properties is available in the literature.

In this study, the Co-free $\text{LaNi}_{4.95}\text{Sn}_{0.3}$ alloy was prepared by vacuum melting followed either by an annealing or by a melt-spinning treatment, the influence of the alloy preparation methods on the crystallographic and electrochemical properties of the alloys was investigated in order to improve the overall electrode properties of the alloys.

2 Experimental

$\text{LaNi}_{4.95}\text{Sn}_{0.3}$ alloy was prepared by vacuum levita-

tion melting in argon atmosphere and remelted three times to ensure a high homogeneity. All starting elemental metals have a purity higher than 99.9%. One-third of the as-cast ingot was annealed under vacuum at 1 223 K for 10 h. Another one-third of the as-cast ingot was remelted and quenched by melt-spinning method. The linear velocity of the rotating copper roller used for the rapid quenching process was 5 m/s.

The alloy samples thus prepared were ground mechanically into powder below 50 μm and used for electrochemical tests and XRD analysis. The crystal structure of the alloy samples was determined by XRD analysis using a Rigaku D/max 2500/PC diffractometer with $\text{CuK}\alpha$ radiation, the XRD patterns were obtained by step scan mode with the step size of $2\theta=0.02^\circ$. These analyses were also made for the hydride samples of the alloys under investigation. To avoid the desorption of hydrogen during measurement, the electrochemically hydrided samples were coated with a glue layer on the sample surface. The composition of the samples was examined by EDS analysis.

For electrochemical tests, pellet type alloy electrodes ($d=10$ mm) were prepared by cold pressing the mixtures of the alloy powder with carbonyl Ni powder in a mass ratio of 1 : 4 and the electrochemical tests were carried out at 298 K in a conventional tri-electrode cell consisting of a working electrode (MH electrode), a sintered $\text{Ni}(\text{OH})_2/\text{NiOOH}$ counter electrode and a Hg/HgO reference electrode, and the electrolyte was 6 mol/L KOH solution. The discharge capacity was determined galvanostatically by using an automatic charge/discharge unit (DC-5). Each electrode was charged at 100 mA/g for 4 h, and discharged at 60 mA/g to the cut-off potential of -0.7 V (vs Hg/HgO). The high rate dischargeability (HRD), defined as $C_n/(C_n+C_{60}) \times 100$, was determined from the ratio of the discharge capacity C_n (with $n=300$ or 600 mA/g, respectively) to the total discharge capacity defined as the sum of C_n and C_{60} , which was the additional capacity measured subsequently at 60 mA/g after C_n was measured. The cycling test was conducted at the charge/discharge current of 300 mA/g. The cycling capacity retention rate S_{200} was defined as $S_{200}=C_{200}/C_{\text{max}} \times 100$, where C_{200} was the discharge capacities at 200th cycles. In evaluating the kinetic properties of the electrodes reaction, the linear polarization curves of the electrode were plotted with a Solarton SI 1287 potentiostat by scanning the electrode potential at the rate of 0.1 mV/s from -5 to $+5$ mV (vs open circuit potential) at 50% depth of discharge (DOD). The potentialstatic discharge technique was used to evaluate the diffusion coefficient of hydrogen within the alloy bulk. After being fully charged followed by a 30 min open circuit rest-period, the test electrodes were

discharged with $+600$ mV potential-step for 5 000 s on a Sloartron SI1287 potentiostat, using the CorrWare electrochemical corrosion software.

3 Results and discussion

Fig.1 shows the XRD patterns of the $\text{LaNi}_{4.95}\text{Sn}_{0.3}$ alloy prepared by three different methods. The lattice parameters of the alloys and their hydrides are listed in Table 1. It is found that the as-cast alloy contains a main phase with CaCu_5 -type structure and a little second phase (Sn), while both the annealed and melt-spun alloys are single phase of CaCu_5 -type structure. In addition, the diffraction peaks for CaCu_5 -type phase become narrower and sharper after the alloy being annealed or rapid quenched, indicating that both the annealed and the melt-spun alloys have a higher crystallinity and relaxed lattice strain. As shown in Table 1, compared with the as-cast alloys, both the annealed and melt-spun alloys show an increase of the value of c/a ratio and cell volume (V), and show a noticeable decrease in the expansion rate of the cell volume ($\Delta V/V$) on hydriding (from 20.6% to the range of 17.7%–18.2%). This result reveals that the cell volume expansion of the alloy induced by hydrogenation can be effectively decreased through the annealing or rapid quenching treatment, which is beneficial to the improvement of the ability of anti-pulverization of the alloys during charge/discharge cycling.

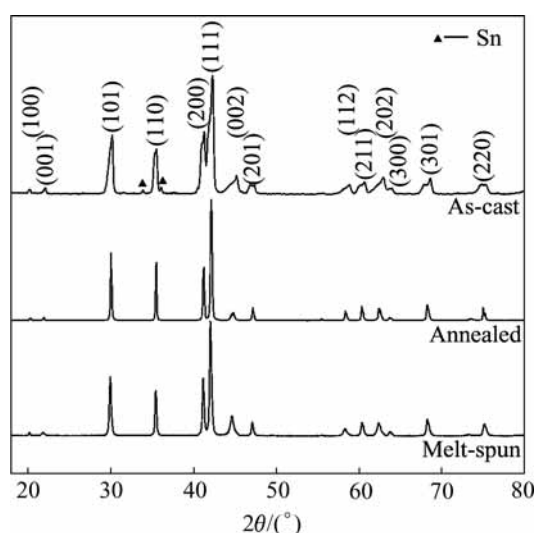


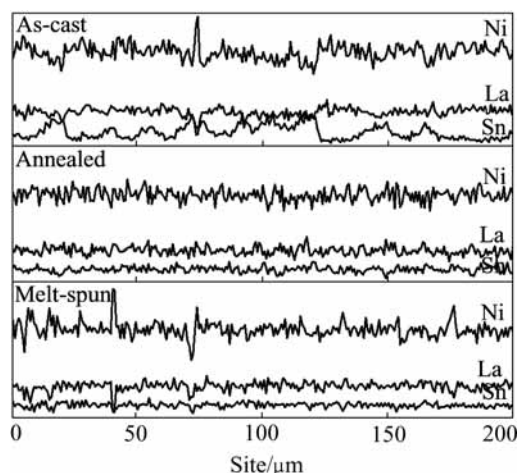
Fig.1 XRD patterns of $\text{LaNi}_{4.95}\text{Sn}_{0.3}$ alloys prepared by three different methods

Fig.2 shows the scanning composition of La, Ni and Sn for sites every 0.77 μm apart along a horizontal straight line on the surface of these alloys by EDS analysis. Compared with the as-cast alloy, it can be seen that the componential fluctuation curves of La, Ni and Sn

Table 1 Lattice parameters of $\text{LaNi}_{4.95}\text{Sn}_{0.3}$ alloys and their hydrides

Sample	Alloy				Hydride				$(\Delta V/V)/\%$
	a/nm	c/nm	V/nm^3	c/a	a/nm	c/nm	V/nm^3	c/a	
As-cast	0.505 4	0.403 3	0.089 21	0.798 0	0.540 0	0.426 0	0.107 55	0.788 9	20.6
Annealed	0.505 9	0.405 0	0.089 76	0.800 5	0.535 8	0.425 1	0.105 67	0.793 4	17.7
Melt-spun	0.504 9	0.405 0	0.089 40	0.802 1	0.535 4	0.425 9	0.105 71	0.795 5	18.2

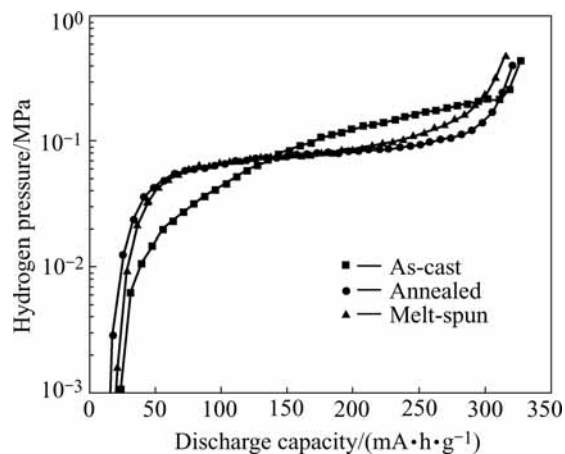
in the annealed and melt spun alloys is more flat, especially the Sn element. This means that the annealing and melt-spinning process effectively improves the compositional homogeneity of the alloy.

**Fig.2** EDS analysis results of Ni, La and Sn distribution in $\text{LaNi}_{4.95}\text{Sn}_{0.3}$ alloys

As shown in Fig.3, the desorption plateaus of the annealed and melt-spun alloys are much flatter and little lower than that of the as-cast alloy, which can be ascribed to their more homogeneous composition and the slightly increase in hydride stability of the alloys. The electrochemical properties of the alloys are summarized in Table 2. It can be seen that the as-cast alloy needs only 2 cycles to reach its maximum discharge capacity (C_{max}) of 326.9 $\text{mA}\cdot\text{h}/\text{g}$, while the activation cycles (N_a) of the annealed and melt-spun alloys increase to 5–6 cycles with a lower discharge capacity of 320.8 $\text{mA}\cdot\text{h}/\text{g}$ and 315.7 $\text{mA}\cdot\text{h}/\text{g}$, respectively.

From Table 2, it is also found that the annealing or melt-spinning treatment results in a decrease of the high-rate dischargeability(HRD), but the HRD of the annealed alloys is higher than that of the melt-spun alloy. At the discharge rate of 300 mA/g , the HRD_{300} of the as-cast alloy is 95.4%, and it decreases to around 90% for the annealed and melt-spun alloys. When the discharge rate increases to 600 mA/g , the HRD_{600} of the as-cast alloy is 85.8%, and it drops to 75.6% and 71.2% for the annealed and melt-spun alloys, respectively.

It is known that the high-rate dischargeability of

**Fig.3** Electrochemical P-C-T curves for hydrogen desorption of $\text{LaNi}_{4.95}\text{Sn}_{0.3}$ alloys at 298 K

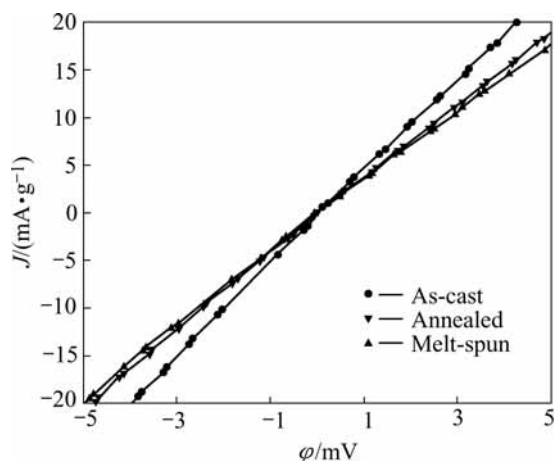
the MH electrode is mainly influenced by the electrochemical reaction rate on the alloy surface and the diffusion rate of hydrogen in the bulk of the alloy[15]. To examine the effect of alloy preparation method on the discharge kinetics, the linear polarization and potential-step experiment were performed on the alloy electrodes. Fig.4 shows the linear polarization curves of the alloy electrodes. The exchange current density J_0 , which is a measure of catalytic activity of the electrode for charge transfer reaction on the alloy surface, was calculated from the slope of polarization curves according to the following equation[15]:

$$J_0 = \left(\frac{RT}{F} \right) \cdot \left(\frac{J}{\eta} \right)_{\eta \rightarrow 0} \quad (1)$$

where J is the applied current density, mA/g ; η is the over-potential, mV ; and R , F , T are the gas constant, Faraday constant and absolute temperature respectively. The exchange current densities J_0 calculated from Eqn.(1) are listed in Table 2. It can be seen that the J_0 value of the as-cast alloy is 123.2 mA/g , and it decreases to 100.1 mA/g and 95.0 mA/g for the annealed and melt-spun alloys respectively, which is consistent with the variation of HRD values of the alloy electrodes. This indicates that the electrochemical reaction rate on the alloy surface slows down slightly after the alloy being annealed or rapidly quenched due to their lower surface electrocatalytic activity, which can be attributed to the decrease

Table 2 Electrochemical properties of LaNi_{4.95}Sn_{0.3} alloys prepared by three methods

Sample	$C_{\max}/(\text{mA}\cdot\text{h}\cdot\text{g}^{-1})$	N_a	HRD/%		$J_0/(\text{mA}\cdot\text{g}^{-1})$	$D/(10^{-10}\text{cm}^2\cdot\text{s}^{-1})$	$S_{200}/\%$
			HRD ₃₀₀	HRD ₆₀₀			
As-cast	326.9	2	95.4	85.8	123.2	3.22	40.1
Annealed	320.8	5	90.9	75.6	100.1	2.47	76.2
Melt-spun	315.7	6	90.1	71.2	95.0	2.38	73.6

**Fig.4** Linear polarization curves of LaNi_{4.95}Sn_{0.3} alloys

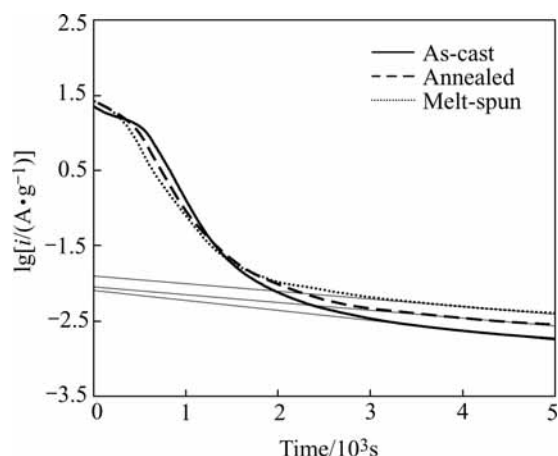
in effective surface area of the alloys as a result of the decreased volume expansion ($\Delta V/V$) on hydriding.

Fig.5 shows the semi-logarithmic plots of anodic current vs time response of the LaNi_{4.95}Sn_{0.3} alloy electrodes. It can be seen that the current-time responses can be divided into two time domains, in the first time region, the oxidation current of hydrogen rapidly declines due to the rapid consumption of hydrogen on the surface. However, in the second time region followed, the current declines more slowly and drops linearly with time. Since hydrogen is supplied from the bulk of the alloy at a rate proportional to the concentration gradient of hydrogen, hence the electrode current is controlled by the diffusion of hydrogen in the second time region. It is reported that in a large anodic potential-step test, after a long discharge time, the diffusion current varies with time according to the following equation[16]:

$$\lg i = \lg \left[\frac{6FD(C_0 - C_s)}{da^2} \right] - \frac{\pi^2}{2.303} \left(\frac{D}{a^2} \right) t \quad (2)$$

where D is the hydrogen diffusion coefficient, cm^2/s ; i the diffusion current density, A/g ; a the radius of spherical alloy particle, cm ; C_0 the initial hydrogen concentration in the alloy bulk, mol/cm^3 ; C_s the hydrogen concentration on the electrode surface, mol/cm^3 ; d the density of the hydrogen storage alloy, g/cm^3 ; t the discharge time, s ; and F the Faraday constant. Thus from the slope of the linear part of the $\lg i$ vs t plot in Fig.5, according to Eqn.(2), D/a^2 can be obtained, and the D value can be estimated if the radius of the alloy particle a is known. Assuming that all the alloys have a

similar particle distribution with an average particle radius of $10 \mu\text{m}$, the hydrogen diffusion coefficient D in the bulk of the alloys was calculated and listed in Table 2. It can be seen that the D value of the as-cast alloy ($3.22 \times 10^{-10} \text{cm}^2/\text{s}$) is slightly larger than that of the annealed and melt-spun alloys ($(2.38\text{--}2.47) \times 10^{-10} \text{cm}^2/\text{s}$), suggesting that the annealing or rapid quenching treatment leads to some decrease in the diffusion rate of hydrogen within the alloy bulk, which agrees with their lower HRD values and the increased hydride stability of the alloys. Therefore, it is believed that the decrease in both the surface electrocatalytic activity and the hydrogen diffusion rate of the annealed and melt-spun alloys is the main cause for their relatively lower high-rate dischargeability.

**Fig.5** Semi-logarithmic plots of anodic current-time responses for LaNi_{4.95}Sn_{0.3} alloys after +600 mV potential-steps at 298 K

The data (S_{200}) of the capacity retention rate of the alloys after 200 cycles are also listed in Table 2. It can be seen that the as-cast alloy shows a rather poor cycling stability. Its discharge capacity reduces to less than half of the initial value after 200 cycles ($S_{200}=40.1\%$) at the charge/discharge rate of $300 \text{mA}/\text{g}$, while the cycling stability of the alloy is improved remarkably by the additional annealing or melt-spun process. The capacity retention rate (S_{200}) of the melt-spun alloy goes up to 73.6% , and increases to 76.2% for the annealed alloy. The great improvement of cycling stability for the annealed and melt-spun alloy can be attributed to their higher homogeneity of composition and the lower volume expansion rate ($\Delta V/V$) of the alloys on hydriding. By using the least square method, the effect of the alloy

preparation methods on the cycling stability (S_{200}) and the cell volume expansion rate ($\Delta V/V$) of the alloys are correlated and shown in Fig.6. It can be seen that the value of S_{200} as a function of the value of $\Delta V/V$ of the alloys shows a nearly linear relationship, indicating that the alloy has a smaller volume expansion and thus an improved cycling stability. It is well accepted that alloy having a smaller volume expansion on hydriding would lead to a lower degree of pulverization and thus exposes less surface area to the corrosive electrolyte, and hence corrodes less and has a better cycling stability[2]. It is thus clear that the annealing and melt-spinning are the effective methods to improve the cycling stability of the Co-free $\text{LaNi}_{4.95}\text{Sn}_{0.3}$ alloy without much detrimental effect on its other electrochemical properties. It can be a good candidate for the low-cost negative electrode materials for Ni/MH batteries.

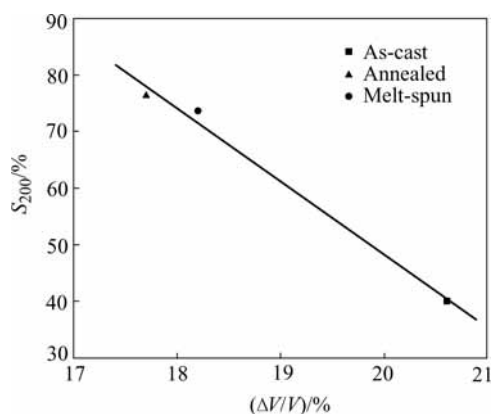


Fig.6 Relation between S_{200} and $\Delta V/V$ of $\text{LaNi}_{4.95}\text{Sn}_{0.3}$ alloys

4 Conclusions

Co-free $\text{LaNi}_{4.95}\text{Sn}_{0.3}$ alloys were prepared by three different processing methods, and their phase structure and electrochemical properties were examined and compared. It is found that the crystallographic and electrochemical properties of the alloys are influenced greatly by the alloy preparation methods. The as-cast alloy consists of a main phase with CaCu_5 -type structure and a few second phase (Sn), has high cell volume expansion rate on hydriding and noticeable element segregation, which all results in a poor cyclic endurance. Annealing or melt-spinning changes the alloy to a single CaCu_5 -type structure phase, lowers the cell volume expansion rate on hydriding and improves the composition homogeneity greatly, leading to a marked improvement in cyclic stability. The activation rate, initial capacity and high-rate dischargeability of the annealed and melt-spun alloys are somewhat lower in comparison with the as-cast alloy. The Co-free $\text{LaNi}_{4.95}\text{Sn}_{0.3}$ alloys prepared by annealing or melt-spinning in this study show a reasonable high capacity

(315.7–320.8 mA·h/g), good cycling stability (S_{200} =73.6%–76.2%) and good 1C rate dischargeability (HRD_{300} ~90%), which is a promising candidate for the low-cost negative electrode materials for Ni/MH batteries.

References

- [1] WILLEMS J J G. Metal hydride electrodes stability of LaNi_5 -related compounds [J]. Philips J Res, 1984, 39(Suppl.1): 54–70.
- [2] REILLY J J, ADZIC G D, JOHNSON J R, et al. The correlation between composition and electrochemical properties of metal hydride electrodes [J]. J Alloys Comp, 1999, 293–295(1–2): 569–582.
- [3] HU W K. Studies on cobalt-free AB_5 -type hydrogen storage alloys [J]. J Alloys Comp, 1999, 289(1–2): 299–305.
- [4] IWAKURA C, OHKAWA K, SENOH H, et al. Electrochemical and crystallographic characterization of Co-free hydrogen storage alloys for use in nickel–metal hydride batteries [J]. Electrochim Acta, 2001, 46(28): 4383–4388.
- [5] MA J X, PAN H G, CHEN C P, et al. The electrochemical properties of Co-free AB_5 type $\text{MnNi}_{(4.45-x)}\text{Mn}_{0.40}\text{Al}_{0.15}\text{Sn}_x$ hydride electrode alloys [J]. J Alloys Comp, 2002, 343: 164–169.
- [6] NOTTEN P H L, EINERHAND R E F, DAAMS J L C. On the nature of the electrochemical cycling stability of non-stoichiometric LaNi_5 -based hydride-forming compounds: Part I Crystallography and electrochemistry[J]. J Alloys Comp, 1994, 210: 221–232.
- [7] ZHANG Shu-kai, LEI Yong-quan, CHEN Li-xin, et al. Electrode characteristics of non-stoichiometric $\text{M}(\text{NiMnAlFe})_x$ alloys[J]. Trans Nonferrous Met Soc China, 2001, 11(2): 183–187.
- [8] LATROCHE M, CHABRE Y, PERCHERON-GUEGAN A, et al. Influence of stoichiometry and composition on the structure and electrochemical properties of AB_{5+y} based alloys used as negative electrode materials in Ni-MH batteries [J]. J Alloys Comp, 2002, 330–332: 787–791.
- [9] CHEN Xian-li, LEI Yong-quan, LIAO Bin, et al. Effects of annealing treatment on microstructure and electrochemical performances of Co-free $\text{MnNi}_{4.6}\text{Al}_{0.3}\text{Si}_{0.1}\text{Fe}_{0.6}$ hydrogen storage alloy [J]. The Chinese Journal of Nonferrous Metals, 2004, 14(11): 1862–1868. (in Chinese)
- [10] MA Z H, QIU J F, CHEN L X, et al. Effects of annealing on microstructure and electrochemical properties of the low Co-containing alloy $\text{M}(\text{NiMnAlFe})_5$ for Ni/MH battery electrode [J]. J Power Sources, 2004, 125(2): 267–272.
- [11] LEI Y Q, ZHANG S K, LU G L, et al. Influence of the material processing on the electrochemical properties of cobalt-free $\text{M}(\text{NiMnAlFe})_5$ alloy [J]. J Alloys Comp, 2002, 330–332: 861–865.
- [12] ANDERY C, BERNARD P, CHANPING Y, et al. Effect of the cooling rate of super-stoichiometric AB_5 alloys with low Co content on their electrochemical performances[J]. J Alloys Comp, 2002, 330–332: 871–874.
- [13] ZHANG S K, SHU K Y, LEI Y Q, et al. The effect of solidification rate on the microstructure and electrochemical properties of Co-free $\text{M}(\text{NiMnAlFe})_5$ alloys[J]. Int J Hydrogen Energy, 2003, 28(9): 977–981.
- [14] VOGT T, REILLY J J, JOHNSON J R, et al. Crystal structure of nonstoichiometric $\text{La}(\text{Ni}, \text{Sn})_{5+x}$ alloys and their properties as metal hydride electrodes[J]. Electrochem Solid-State Lett, 1999, 2(3): 111–114.
- [15] IWAKURA C, OURA T, INOUSE H, et al. Effects of substitution with foreign metals on the crystallographic, thermodynamic and electrochemical properties of AB_5 -type hydrogen storage alloys[J]. Electrochim Acta, 1996, 41(1): 117–121.
- [16] ZHENG G, DOPOV B N, WHITE R E. Electrochemical determination of the diffusion coefficient of hydrogen through an $\text{LaNi}_{4.25}\text{Al}_{0.75}$ electrode in alkaline aqueous solution[J]. J Electrochem Soc, 1995, 142(8): 2695–2698.

(Edited by YUAN Sai-qian)